Identification and Vitro Validation of Biomarkers with Diagnostic and Prognostic for Lung Squamous Cell Carcinoma

Xiaopeng Zhao
Hebei Medical University Fourth Affiliated Hospital
Fan Yu
Hebei Medical University Fourth Affiliated Hospital
Xu He
Hebei Medical University Fourth Affiliated Hospital
Miao Wang
Hebei Medical University Fourth Affiliated Hospital
Haoran Zhang
Hebei Medical University Fourth Affiliated Hospital
Xuefeng Zhang
Hebei Medical University Fourth Affiliated Hospital
Hongyan Wang (HongyanWang_doctor@163.com)
Hebei Medical University Fourth Affiliated Hospital https://orcid.org/0000-0003-2535-6073

Research

Keywords: lung squamous cell carcinoma, RNA sequencing, DEmRNAs, DElncRNAs, DElncRNA-DEmRNA coexpression

Posted Date: September 22nd, 2021

DOI: https://doi.org/10.21203/rs.3.rs-907830/v1

Version of Record: A version of this preprint was published at Journal of Thoracic Disease on January 1st, 2021. See the published version at https://doi.org/10.21037/jtd-22-343.

Abstract

Background: This study aimed to find biomarkers with diagnostic and prognostic for lung squamous cell carcinoma and to validate key biomarkers in vitro

Methods: RNA sequencing was used to identify differentially expressed mRNAs (DEmRNAs) and lncRNAs (DElncRNAs) between LUSC and normal tissue. Using published dataset, we also validated the result of RNA sequencing. The diagnostic and prognostic value of candidate genes were evaluated by ROC curve analysis and survival analysis, respectively. To uncover the confirm effect of MIR205HG in LUSC, we knocked down MIR205HG expression in NCI-H520 cells. Then, MTT assay and transwell assay was used to detect the effect of MIR205HG on cell proliferation and migration.

Rsults: In total, 1946 DEmRNAs and 428 DElncRNAs were identified in LUSC compared to normal tissues. A total of 147 DElncRNAs-nearby target DEmRNAs pairs and 851 DElncRNA-DEmRNA co-expression pairs were obtained. Except for NEAT1, expression of the others in the The Cancer Genome Atlas (TCGA) results was consistent with our RNA sequencing, generally. ROC curve analysis displayed that the MCM2, SERPINB5, ITGB8, CASC19 and MIR205HG could predict the occurrence of LUSC. Survival analysis suggested that SERPINB5, NEAT1 and MIR205HG had potential prognostic value for LUSC. Knockdown of MIR205HG inhibits cell proliferation and migration in NCI-H520 cell. In addition, knockdown of MIR205HG significantly reduced the expression of ITGB8.

Conclusions: This data may contribute to uncover the pathogenesis of LUSC and provide new and accurate therapeutic targets for LUSC.

Introduction

Background

Lung cancer, as a most commonly diagnosed malignancy, is one of the leading causes of cancer death global.[1] Non-small cell lung cancer is the major subtype of lung cancer, lung squamous cell carcinoma (LUSC) as a most frequent subtype of non-small cell lung cancer, accounting for approximately 40% of the diagnosed cases of lung cancer each year.[2] Currently, the main treatment strategies for LUSC including surgery, radiotherapy and chemotherapy.[3] However, the 5-year overall survival rate for LUSC patients remains unsatisfactory. This is largely due to the limited understanding molecular mechanisms of LUSC in existing studies.[4, 5] Thence, it is extremely critical to find effective and promising biomarkers for LUSC patients.

Long noncoding RNA (lncRNA), with more than 200 nucleotides base long, drawn increasing attention and has been widely associated with multiple diseases.[6, 7] With the emergence of sequencing technology, bioinformatics have become most frequently used means to find potential biomarkers in various diseases, and the possible function of lncRNA in multiple diseases is being fully studied.[8, 9]

Interestingly, a growing body of studies has uncovered that dysregulation of LncRNAs is associated with occurrence and progression of a variety of cancer.[9, 10] Until now, the function of lncRNAs in underlying pathogenesis of LUSC is not fully illuminated. Therefore, it is important to expand our understanding of the pathogenesis of LUSC and screen novel biomarkers to improve treatment strategies of LUSC.

In this study, we applied the RNA sequencing to filtrate the differential expression mRNA (DEmRNAs) and differential expression lncRNAs (DElncRNAs) in LUSC versus normal control. Moreover, functional annotation and protein-protein interaction (PPI) network of DEmRNAs were performed. DEmRNA-DElncRNA interaction analysis and functional annotation of DEmRNAs co-expressed with DElncRNAs were also structured. The diagnostic and prognostic value of candidate genes were evaluated. The goal of our work is to better uncover the underlying mechanisms of LUSC and find novel and accurate biomarkers for LUSC.

Methods

Patients

Three lung squamous cell carcinoma (LUSC) patients were included in this study. The 6 tissue samples (3 LUSC samples and 3 paired adjacent normal samples) were utilized to carry out the RNA sequencing. Each patient submitted the signed informed consents, and this study were approved by the ethical committee of our hospital.

RNA isolation and sequencing

Total RNA was extracted from samples using the Trizol kit (Invitrogen, Carlsbad, CA, USA). Total RNA was further purifed with the Ribo-Zero Magnetic kit (EpiCentre, Madison, WI, USA). Illumina Hiseq Xten platform (Illumina, San Diego, CA, USA) was performed to conduct sequencing of mRNA. xpression levels of lncRNA and mRNA were compared using edgeR (http://www.bioconductor.org/packages/release/bioc/html/edgeR.html). MRNA and lncRNAs with |log2FC|>1 and p value<0.05 was defined as significant DEmRNAs and DElncRNAs. Volcano plot was generated in R package (https://www.r-project.org/). Hierarchical clustering analysis of top 100 DEmRNAs and DElncRNAs was structured by heatmap.2 (http://127.0.0.1:28428/library/gplots/html/heatmap.2.html).

Functional annotation

Gene Ontology (GO) classification and Kyoto Encyclopedia of Genes and Genomes (KEGG) pathway enrichment analysis were retrieved via GeneCoDis3 (http://genecodis.cnb.csic.es/analysis). Significantly enrichment was defined by p value <0.05.

PPI network construction

The top 50 up-regulated and down-regulated DEmRNAs were applied to establish the PPI network using BioGRID and Cytoscape 3.6.1 (http://www.cytoscape.org/). The nodes and edges to represent the proteins and interactions between two proteins, respectively.

DEmRNA-DElncRNA interaction analysis

To study the nearby DEmRNAs of DElncRNAs with cis-regulatory effects, DEmRNAs transcribed within a 100 kb window up- or down-stream of DElncRNAs between LUSC and normal controls were sought. Furthermore, the DEmRNAs co-expressed with DElncRNAs were screened as well. The pairwise Pearson correlation coefficients between DEmRNAs and DElncRNAs were analyzed. DElncRNA-DEmRNA pairs with $p<0.001$ and $|r| \geq 0.999$ were served as significant mRNA-lncRNA co-expression pairs.

Validation in The Cancer Genome Atlas (TCGA)

The expression pattern of selected DEmRNAs and DElncRNAs were validated with TCGA dataset.
We downloaded from the TCGA dataset, which consisted of 501 patients with LUSC and 49 normal controls.

Receiver operating characteristic (ROC) curve analyses

In order to evaluate the diagnostic value of DEmRNAs and DElncRNAs in LUSC, the “pROC” package was performed to generate ROC, and the area under the ROC curve (AUC) represents the diagnostic value. When AUC value was greater than 0.8, the DEG was is thought to be able to distinguish between case and normal controls with good specificity and sensitivity.

Survival analysis

To evaluate the prognostic of candidate genes, survival analysis was generated using clinical data from TCGA. Kaplan–Meier curve was plotted using the survival (https://cran.r-project.org/web/packages/survival/index.html) in R.

Cell culture and Cell transfection

Human lung squamous cell carcinoma cell lines NCI-H520 were obtained from American Type Culture Collection (ATCC, Manassas, VA, USA) and cultured in endothelial cell growth medium (Gibco, Rockville, MD, USA) supplemented with 10% fetal bovine serum (Gibco) in 5% CO_2 at 37 °C. Small interfering RNA

targeting MIR205HG (si-MIR205HG) and scramble siRNA of MIR205HG (si-NC) were purchased by Guangzhou Ribobio (Guangzhou, China). For transfection, NCI-H520 cells were inoculated with 60 %-70 % fusion and allowed to adhere overnight. Subsequently, the corresponding plasmid was then transfected into the cells by Lipofectamine 2000 according to the manufacturer's instructions. After 48h, cells were collected for subsequent experiments.

CCK8

Cell viability was measured using CCK8 kit (CCK-8 reagent). In brief, the treated NCI-H520 cells were inoculated on 96-well plates for 12 h, and 10 uLCCK-8 reagent was added to each well for 37°C for 4 h. The absorbance value of each well at 450 nm was determined using a microplate reader.

Transwell assay

Cell migration capacities were detected using by transwell assays. Cells resuspended in serum-free medium were placed into the upper chamber of a 24-Transwell plate with 8 μm pore filter (BD Biosciences, Franklin Lakes, NJ, USA).Then, 500 μl of growth medium containing 10% FBS was added into lower chamber. After incubation for 24 h, the cells that moved through the underside of the membrane filter were fixed with 4% paraformaldehyde and stained with 0.25% crystal violet. The number of migrated or invaded cells was counted and the images were photographed under a light microscope (Olympus, Tokyo, Japan).

Real-time quantitative RT-PCR

Total RNA was isolated from NCI-H520 cells using a RNA simple total RNA kit Tiangen, Beijing, China) and then reverse-transcribed with the Fast Quant RT Kit (Tiangen) according to the manufacturer's instructions. Quantitative real-time PCR were performed using the Super Real PreMix Plus SYBR Green (Tiangen) on a QuantStudio 6 Flex system. The relative quantification of genes was calculated using $2^{-\Delta\Delta Ct}$ method.

Western blot

Cells were lysed with RIPA buffer (Beyotime, Shanghai, China), and total protein was obtained. The protein concentration was measured using the BCA protein assay kit (Tiangen). After processing with loading buffer, proteins (50 μg) were subjected to SDS/PAGE (10-12% gels), and then transferred to PVDF membranes (Millipore, Billerica, MA, USA). The blot was blocked with 5% nonfat milk for 2 h at room temperature and incubated primary antibodies overnight at 4°C. After washing, blots were incubated with appropriate HRP-conjugated secondary antibody for 2 h. The protein bands were visualized revealed by chemiluminescence using an ECL detection kit (Millipore).

Results

DEmRNAs and DElncRNAs in LUSC

Base on the thresholds of |log2FC|>1 and p value<0.05, a total of 1946 DEmRNAs (940 down-regulated and 1006 up-regulated mRNAs) and 428 DElncRNAs (206 down-regulated and 222 up-regulated lncRNAs) between LUSC and normal tissue were obtained. As shown in Figure 1, the volcano plot shows the overall distribution of DEmRNAs and DElncRNAs. Hierarchical clustering analysis of top 100 DEmRNAs and DElncRNAs was exhibited in Figure 2A and Figure 2B, respectively. Circus plots representing the distribution of DElncRNAs and DEmRNAs on chromosomes (Figure 2C).

Functional annotation of DEmRNAs

GO and KEGG enrichment analysis were used to uncover the biological function of DEmRNAs. GO enrichment analysis results revealed that mitotic cell cycle (p=1.54E-31), cell adhesion (FDR=2.71E-31), cytoplasm (FDR=2.19E-84), protein binding (FDR=9.16E-83) and nucleotide binding (FDR=4.84E-37) were significantly enriched GO terms (Figure 3A-C). Through KEGG enrichment analysis, cell cycle (FDR=8.23E-17), pathways in cancer (FDR=8.41E-12), p53 signaling pathway (FDR=9.51E-10), ECM-receptor interaction (FDR=9.75E-09), DNA replication (FDR=1.11E-08) and MAPK signaling pathway (FDR=1.47E-08) were significantly enriched pathways (Figure 3D).

PPI network

The PPI network of top 50 up- and down-regulated DEmRNAs were consisted of 255 nodes and 253 edges (Figure 4). TP63 (Degree=21), TRIM29 (Degree=15), FOS (Degree=13), MCM2 (Degree=12), LRRK2 (Degree=11), NR4A1 (Degree=9), HIST2H3C (Degree=9), CALML3 (Degree=8), HBB (Degree=7), PKP1 (Degree= 7) and SERPINB5 (Degree=7) were considered the hub proteins.

DEmRNA-DElncRNA interaction analysis

A total of 147 DElncRNAs-nearby target DEmRNAs pairs were obtained which were consisted of 98 DElncRNAs and 128 DEmRNAs (Figure 5). In total, 851 DElncRNA-DEmRNA co-expression pairs including 213 DElncRNAs and 377 DEmRNAs were identified with absolute value of the | r |< 0.999 and p-value<0.01 (Figure 6).

Functional annotation of DEmRNAs co-expressed with DElncRNAs

GO enrichment analysis results revealed that cellular response to hypoxia (p=2.82E-09), cell adhesion (FDR=6.18E-08), plasma membrane (FDR=3.02E-16), protein binding (FDR=1.27E-18) and receptor binding (FDR=9.98E-09) were significantly enriched GO terms (Figure 7A-C). Base on KEGG enrichment analysis, Cell cycle (FDR=3.57E-05), cell adhesion molecules (FDR=4.00E-05), p53 signaling pathway (FDR=5.71E-04), ECM-receptor interaction (FDR=1.59E-03), small cell lung cancer (FDR=1.59E-03) and focal adhesion (FDR=3.89E-03) were significantly enriched pathways (Figure 7D).

Validation in the TCGA dataset

The expression pattern of selected of 3 DEmRNAs (MCM2, SERPINB5 and ITGB8) and 3 DElncRNAs (NEAT1, CASC19 and MIR205HG) were validated in LUSC. As displayed in Figure 8, NEAT1 was down-regulated, which was inconsistent with our integration results. MCM2, SERPINB5, ITGB8, CASC19and MIR205HG were up-regulated in LUSC, which was consistent with our integration results, suggesting that the results were convincing.

ROC curve analyses

As shown in Figure 9, MCM2 (AUC=0.997), SERPINB5 (AUC=0.979), ITGB8 (AUC=0.913), CASC19 (AUC=0.898) and MIR205HG (AUC=0.961) were capable of discriminating LUSC and normal controls, and NEAT1 (AUC=0.574) was not capable of discriminating LUSC and normal controls.

Survival analysis

We assess the prognostic value of 3 DEmRNAs (MCM2, SERPINB5 and ITGB8) and 3 DElncRNAs (NEAT1, CASC19 and MIR205HG) in LUSC.Among which, SERPINB5, NEAT1 and MIR205HG were associated with the survival of patients with LUSC (Figure 10).

Knockdown of MIR205HG inhibits NCI-H520 cell proliferation and migration

To further uncover the confirm effect of MIR205HG in LUSC, we adopted NCI-H520 to knock down MIR205HG. qRT-PCR was used to measure the relative mRNA expression of MIR205HG in NCI-H520 cells. As shown in Figure 11A, the expression of MIR205HG was markedly decreased in the si-MIR205HG group than in the empty vector group. Then, MTT assay and transwell assay was used to detect the effect of MIR205HG on cell proliferation and migration, respectively. Knockdown of MIR205HG remarkably inhibited proliferation and migration of NCI-H520 cells (Figure 11B and C). In addition, knockdown of MIR205HG significantly reduced the expression of ITGB8 (Figure 11D). In conclusion, these results

suggest that Knockdown of MIR205HG inhibits cell proliferation and migration in LUSC, and MIR205HG may be a new target for the treatment of LUSC.

Discussion

Although the occurrence rate of LUSC is falling, it remains the cause of the highest cancer-related death [1]. To date, the RNA sequencing data analysis elated to the expression profile of lncRNA in LUSC remain scarce.[11] In order to reveal the pathogenesis, the RNA sequencing were utilized to acquire DEmRNAs and DElncRNAs between LUSC and normal control. In total, 1946 DEmRNAs (940 down-regulated and 1006 up-regulated mRNAs) and 428 DElncRNAs (206 down-regulated and 222 up-regulated lncRNAs) between LUSC and normal tissue were obtained. Functional annotation of DEmRNAs results showed that cell cycle, pathways in cancer, p53 signaling pathway, ECM-receptor interaction, DNA replication and MAPK signaling pathway were significantly enriched pathways. PPI network and DEmRNA-DElncRNA interaction analysis were performed. Base on the functional annotation of DEmRNAs co-expressed with DElncRNAs, cell cycle, cell adhesion molecules, p53 signaling pathway, ECM-receptor interaction, small cell lung cancer and focal adhesion were significantly enriched pathways.

MCM2 belongs to the MCM family and has been identified as a biomarkers for the progression and prognosis of several types of human cancers.[12] MCM2 is highly expressed in a variety of human cancers, including breast cancer, stomach cancer, colorectal cancer, lung cancer, hepatocellular carcinoma and other human tumors.[13–19] Wu et al. reported that the expression level of MCM2 was up-regulated in LUSC tissues and cell lines, and MCM2 was markedly related to low overall survival of patients with LUSC.[14] Herein, we performed RNA sequencing, and displayed MCM2 expression was elevated between LUSC tissues and adjacent normal. Base on PPI network, MCM2 was one of hub proteins in LUSC and significantly enriched in cell cycle pathway. Therefore, we supposed that MCM2 involved the occurrence and development of LUSC by regulating cell cycle pathway.

Serpin family B member 5 (SERPINB5), a member of the serpin superfamily, is a serine protease inhibitor that suppresses tumor progression and metastasis.[20–22] Higher SERPINB5 expression has been also reported to be associated with better prognosis for non-small cell lung cancer, esophageal squamous cell carcinoma, ovarian cancer and bladder cancer.[23–26] In this study, SERPINB5 expression was increased in LUSC tissues compared to adjacent normal. SERPINB5, as one of hub proteins, was significantly enriched in p53 signaling pathway. Isoalantolactone regulated cell cycle arrest and apoptosis of LUSC cells by activating of p53 signaling pathway.[27] Thence, we speculated that SERPINB5 involved the occurrence and development of LUSC by regulating p53 signaling pathway.

Nuclear paraspeckle assembly transcript 1 (NEAT1) is a newly lncRNA which has been shown to be abnormally elevated in in a variety of human cancer.[28] Recently, more and more attention has been paid towards the study of NEAT1, which has been found to be involved in the occurrence and development of non-small cell lung cancer through targeting miRNAs and regulating multiple signaling pathways.[29–32]

CASC19 is a novel found lncRNA located on 8q24 region of the chromosome.[33] CASC19 has been reported to be increased in non-small cell lung cancer tissues and cell lines, and CASC19 accelerates the cell proliferation, migration and invasive capacities of non-small cell lung cancer by regulating miRNA-130b-3p.[34] Here, NEAT1 and CASC19 were also increased in LUSC tissues compared to adjacent normal. According to these studies, we speculated that NEAT1 and CASC19 involved the occurrence and progress of LUSC.

LncRNAMIR205 host gene (MIR205HG) is a novel discovered LncRNA involved in the regulation of various cancer cell processes. Overexpression of MIR205HG has been reported to be connected with tumor progression of esophageal cancer, ovarian and lung cancer.[35–37] MIR205HG depletes miR-590-3p leading unlimited grow of head and neck squamous cell carcinoma cells.[38] MIR205HG, as a ceRNA (competitive endogenous RNA), accelerate tumor proliferation and progression in cervical cancer by targeting mir-122-5p.[39] MIR205HG regulated cell proliferation, apoptosis and migration of cervical cancer cells by modulating SRSF1 and KRT17.[40] In the current study, MIR205HG was increased in LUSC tissues compared to adjacent normal. Through the DElncRNAs-DEmRNAs interaction network, ITGB8 were co-expression with MIR205HG. ITGB8 was significantly enriched in pathway of ECM-receptor interaction, cell adhesion molecules and focal adhesion. In our study, knockdown of MIR205HG inhibits cell proliferation and migration in LUSC. In addition, knockdown of MIR205HG significantly reduced the expression of ITGB8. These results indicated that MIR205HG inhibits LUSC cell proliferation and migration by modulating the expression of ITGB8.

Conclusions

In summary, we identified 1946 DEmRNAs and 428 DElncRNAs in LUSC compared to normal tissues. Cell cycle, pathways in cancer, p53 signaling pathway, ECM-receptor interaction, DNA replication and MAPK signaling pathway were significantly enriched pathways of DEmRNAs. Base on the PPI network, TP63, TRIM29, FOS, MCM2, LRRK2, NR4A1, HIST2H3C, CALML3, HBB, PKP1 and SERPINB5 were considered the hub proteins. In total, 147 DElncRNAs-nearby target DEmRNAs pairs and 851 DElncRNAs-DEmRNAs co-expression pairs were obtained. Cell cycle, cell adhesion molecules, p53 signaling pathway, ECM-receptor interaction, small cell lung cancer and focal adhesion were significantly enriched pathways of DEmRNAs co-expressed with DElncRNAs. Except for NEAT1, expression of the others in the The Cancer Genome Atlas (TCGA) results was consistent with that in our RNA sequencing, generally. ROC curve analysis displayed that the MCM2, SERPINB5, ITGB8, CASC19 and MIR205HG could predict the occurrence of LUSC. Survival analysis suggested that SERPINB5, NEAT1 and MIR205HG had potential prognostic value for LUSC. This findings may contribute to recognize the mechanisms of LUSC and the exploit of treatment targets for LUSC. Some limitations of our study should be mentioned. More samples are needed to validate expression of mRNAs and lncRNAs. Furthermore, more experiments in vivo and in vitro were used to reveal the biological functions of mRNAs and lncRNAs in LUSC.

Abbreviations

Differentially expressed mRNAs DEmRNAs

LncRNAs DElncRNAs

The Cancer Genome Atlas TCGA

Lung squamous cell carcinoma LUSC

Long noncoding RNA lncRNA

Nuclear paraspeckle assembly transcript 1 NEAT1

ceRNA competitive endogenous RNA

Serpin family B member 5 SERPINB5

Nuclear paraspeckle assembly transcript 1 NEAT1

Serpin family B member 5 SERPINB5

Receiver operating characteristic ROC

Serpin family B member 5 SERPINB5

Validation in The Cancer Genome Atlas TCGA

Receiver operating characteristic ROC

Area under the ROC curve AUC

American Type Culture Collection ATCC,

Declarations

Ethics approval and consent to participate

This study was approved by the ethical committee of the fourth hospital of hebei medical university. Written informed consent was obtained from all participants.

Consent for publication

The subjects gave written informed consent for the publication of any associated data.

Availability of data and materials

The dataset supporting the conclusions of this article is included within the article.

Competing Interests

The authors declare that they have no conflict of interest.

Funding

None.

Author contributions

Hongyan Wang and Xiaopeng Zhao contributed to the conception of the study. Fan Yu, Xu He and Miao Wang contributed the materials and performed the experiment. Haoran Zhang and Xuefeng Zhang performed the data analyses. Hongyan Wang and Xiaopeng Zhao contributed significantly in writing the manuscript. All authors read and approved the final manuscript.

Acknowledgements

None.

References

1. Ferlay J, Soerjomataram I, Dikshit R, Eser S, Mathers C, Rebelo M, et al. Cancer incidence and mortality worldwide: sources, methods and major patterns in GLOBOCAN 2012. Int J Cancer. 2015;136:E359–86. https://doi:10.1002/ijc.29210.
2. Piperdi B, Merla A, Perez-Soler R. Targeting angiogenesis in squamous non-small cell lung cancer. Drugs. 2014;74:403–13. https://doi:10.1007/s40265-014-0182-z.
3. Wang Z, Niu X, Liu J, Chen L, Qin B. Identification of seven-gene signature for prediction of lung squamous cell carcinoma. Onco Targets Ther. 2019;12:5979–88. https://doi:10.2147/ott.s198998.
4. Guo T, Li J, Zhang L, Hou W, Wang R, Zhang J, et al. Multidimensional communication of microRNAs and long non-coding RNAs in lung cancer. J Cancer Res Clin Oncol. 2019;145:31–48. https://doi:10.1007/s00432-018-2767-5.
5. Choi M, Kadara H, Zhang J, Parra ER, Rodriguez-Canales J, Gaffney SG, et al. Mutation profiles in early-stage lung squamous cell carcinoma with clinical follow-up and correlation with markers of immune function. Ann Oncol. 2017;28:83–9. https://doi:10.1093/annonc/mdw437.
6. Liu Y, Liu B, Jin G, Zhang J, Wang X, Feng Y, et al. An Integrated Three-Long Non-coding RNA Signature Predicts Prognosis in Colorectal Cancer Patients. Front Oncol. 2019;9:1269. https://doi:10.3389/fonc.2019.01269.
7. Zhao Y, Zhang Y, Zhang L, Dong Y, Ji H, Shen L. The Potential Markers of Circulating microRNAs and long non-coding RNAs in Alzheimer's Disease. Aging Dis. 2019;10:1293–301. https://doi:10.14336/ad.2018.1105.

8. Wang Y, Wu N, Liu J, Wu Z, Dong D. FusionCancer: a database of cancer fusion genes derived from RNA-seq data. Diagn Pathol. 2015;10:131. https://doi:10.1186/s13000-015-0310-4.
9. Jiao Y, Li Y, Ji B, Cai H, Liu Y. Clinical Value of lncRNA LUCAT1 Expression in Liver Cancer and its Potential Pathways. J Gastrointestin Liver Dis. 2019;28:439–47. https://doi:10.15403/jgld-356.
10. Chen S, Liu Y, Wang Y, Xue Z. LncRNA CCAT1 Promotes Colorectal Cancer Tumorigenesis Via A miR-181b-5p/TUSC3 Axis. Onco Targets Ther. 2019;12:9215–25. https://doi:10.2147/ott.s216718.
11. Li R, Yang YE, Jin J, Zhang MY, Liu X, Liu XX, et al. Identification of lncRNA biomarkers in lung squamous cell carcinoma using comprehensive analysis of lncRNA mediated ceRNA network. Artif Cells Nanomed Biotechnol. 2019;47:3246–58. https://doi:10.1080/21691401.2019.1647225.
12. Simon NE, Schwacha A. The Mcm2-7 replicative helicase: a promising chemotherapeutic target. Biomed Res Int. 2014;2014:549719. https://doi:10.1155/2014/549719.
13. Sun M, Wu G, Li Y, Fu X, Huang Y, Tang R, et al. Expression profile reveals novel prognostic biomarkers in hepatocellular carcinoma. Front Biosci (Elite Ed). 2010;2:829–40. https://doi:10.2741/e144.
14. Wu W, Wang X, Shan C, Li Y, Li F. Minichromosome maintenance protein 2 correlates with the malignant status and regulates proliferation and cell cycle in lung squamous cell carcinoma. Onco Targets Ther. 2018;11:5025–34. https://doi:10.2147/ott.s169002.
15. Hanna-Morris A, Badvie S, Cohen P, McCullough T, Andreyev HJ, Allen-Mersh TG. Minichromosome maintenance protein 2 (MCM2) is a stronger discriminator of increased proliferation in mucosa adjacent to colorectal cancer than Ki-67. J Clin Pathol. 2009;62:325–30. https://doi:10.1136/jcp.2007.054643.
16. Yang C, Wen Y, Li H, Zhang D, Zhang N, Shi X, et al. Overexpression of minichromosome maintenance 2 predicts poor prognosis in patients with gastric cancer. Oncol Rep. 2012;27:135–42. https://doi:10.3892/or.2011.1473.
17. Tokes T, Tokes AM, Szentmartoni G, Kiszner G, Madaras L, Kulka J, et al. Expression of cell cycle markers is predictive of the response to primary systemic therapy of locally advanced breast cancer. Virchows Arch. 2016;468:675–86. https://doi:10.1007/s00428-016-1925-x.
18. Zhong H, Chen B, Neves H, Xing J, Ye Y, Lin Y, et al. Expression of minichromosome maintenance genes in renal cell carcinoma. Cancer Manag Res. 2017;9:637–47. https://doi:10.2147/cmar.s146528.
19. Huang B, Hu B, Su M, Tian D, Guo Y, Lian S, et al. Potential role of minichromosome maintenance protein 2 as a screening biomarker in esophageal cancer high-risk population in China. Hum Pathol. 2011;42:808–16. https://doi:10.1016/j.humpath.2010.04.022.
20. Nam E, Park C. Maspin suppresses survival of lung cancer cells through modulation of Akt pathway. Cancer Res Treat. 2010;42:42–7. https://doi:10.4143/crt.2010.42.1.42.
21. Snoeren N, Emmink BL, Koerkamp MJ, van Hooff SR, Goos JA, van Houdt WJ, et al. Maspin is a marker for early recurrence in primary stage III and IV colorectal cancer. Br J Cancer. 2013;109:1636–47. https://doi:10.1038/bjc.2013.489.

22. Joensuu KM, Leidenius MH, Andersson LC, Heikkila PS. High expression of maspin is associated with early tumor relapse in breast cancer. Hum Pathol. 2009;40:1143–51. https://doi:10.1016/j.humpath.2009.02.006.
23. Klasa-Mazurkiewicz D, Narkiewicz J, Milczek T, Lipinska B, Emerich J. Maspin overexpression correlates with positive response to primary chemotherapy in ovarian cancer patients. Gynecol Oncol. 2009;113:91–8. https://doi:10.1016/j.ygyno.2008.12.038.
24. Wang Y, Sheng S, Zhang J, Dzinic S, Li S, Fang F, et al. Elevated maspin expression is associated with better overall survival in esophageal squamous cell carcinoma (ESCC). PLoS One. 2013;8:e63581. https://doi:10.1371/journal.pone.0063581.
25. Takanami I, Abiko T, Koizumi S. Expression of maspin in non-small-cell lung cancer: correlation with clinical features. Clin Lung Cancer. 2008;9:361–6. https://doi:10.3816/CLC.2008.n.052.
26. Kramer MW, Waalkes S, Hennenlotter J, Serth J, Stenzl A, Kuczyk MA, et al. Maspin protein expression correlates with tumor progression in non-muscle invasive bladder cancer. Oncol Lett. 2010;1:621–6. https://doi:10.3892/ol_00000110.
27. Jin C, Zhang G, Zhang Y, Hua P, Song G, Sun M, et al. Isoalantolactone induces intrinsic apoptosis through p53 signaling pathway in human lung squamous carcinoma cells. PLoS One. 2017;12:e0181731. https://doi:10.1371/journal.pone.0181731.
28. Yu X, Li Z, Zheng H, Chan MT, Wu WK. NEAT1: A novel cancer-related long non-coding RNA. Cell Prolif 2017;50 https://doi:10.1111/cpr.12329.
29. Sun C, Li S, Zhang F, Xi Y, Wang L, Bi Y, et al. Long non-coding RNA NEAT1 promotes non-small cell lung cancer progression through regulation of miR-377-3p-E2F3 pathway. Oncotarget. 2016;7:51784–814. https://doi:10.18632/oncotarget.10108.
30. Sun SJ, Lin Q, Ma JX, Shi WW, Yang B, Li F. Long non-coding RNA NEAT1 acts as oncogene in NSCLC by regulating the Wnt signaling pathway. Eur Rev Med Pharmacol Sci. 2017;21:504–10.
31. Li S, Yang J, Xia Y, Fan Q, Yang KP. Long Noncoding RNA NEAT1 Promotes Proliferation and Invasion via Targeting miR-181a-5p in Non-Small Cell Lung Cancer. Oncol Res. 2018;26:289–96. https://doi:10.3727/096504017x15009404458675.
32. Jiang P, Chen A, Wu X, Zhou M, Ul Haq I, Mariyam Z, et al. NEAT1 acts as an inducer of cancer stem cell-like phenotypes in NSCLC by inhibiting EGCG-upregulated CTR1. J Cell Physiol. 2018;233:4852–63. https://doi:10.1002/jcp.26288.
33. Teerlink CC, Leongamornlert D, Dadaev T, Thomas A, Farnham J, Stephenson RA, et al. Genome-wide association of familial prostate cancer cases identifies evidence for a rare segregating haplotype at 8q24.21. Hum Genet. 2016;135:923–38. https://doi:10.1007/s00439-016-1690-6.
34. Qu CX, Shi XC, Zai LQ, Bi H, Yang Q. LncRNA CASC19 promotes the proliferation, migration and invasion of non-small cell lung carcinoma via regulating miRNA-130b-3p. Eur Rev Med Pharmacol Sci. 2019;23:247–55. https://doi:10.26355/eurrev_201908_18654.
35. Iorio MV, Visone R, Di Leva G, Donati V, Petrocca F, Casalini P, et al. MicroRNA signatures in human ovarian cancer. Cancer Res. 2007;67:8699–707. https://doi:10.1158/0008-5472.can-07-1936.

36. Hezova R, Kovarikova A, Srovnal J, Zemanova M, Harustiak T, Ehrmann J, et al. MiR-205 functions as a tumor suppressor in adenocarcinoma and an oncogene in squamous cell carcinoma of esophagus. Tumour Biol. 2016;37:8007–18. https://doi:10.1007/s13277-015-4656-8.
37. Zarogoulidis P, Petanidis S, Kioseoglou E, Domvri K, Anestakis D, Zarogoulidis K. MiR-205 and miR-218 expression is associated with carboplatin chemoresistance and regulation of apoptosis via Mcl-1 and Survivin in lung cancer cells. Cell Signal. 2015;27:1576–88. https://doi:10.1016/j.cellsig.2015.04.009.
38. Di Agostino S, Valenti F, Sacconi A, Fontemaggi G, Pallocca M, Pulito C, et al. Long Non-coding MIR205HG Depletes Hsa-miR-590-3p Leading to Unrestrained Proliferation in Head and Neck Squamous Cell Carcinoma. Theranostics. 2018;8:1850–68. https://doi:10.7150/thno.22167.
39. Li Y, Wang H, Huang H. Long non-coding RNA MIR205HG function as a ceRNA to accelerate tumor growth and progression via sponging miR-122-5p in cervical cancer. Biochem Biophys Res Commun. 2019;514:78–85. https://doi:10.1016/j.bbrc.2019.04.102.
40. Dong M, Dong Z, Zhu X, Zhang Y, Song L. Long non-coding RNA MIR205HG regulates KRT17 and tumor processes in cervical cancer via interaction with SRSF1. Exp Mol Pathol. 2019;111:104322. https://doi:10.1016/j.yexmp.2019.104322.

Figures

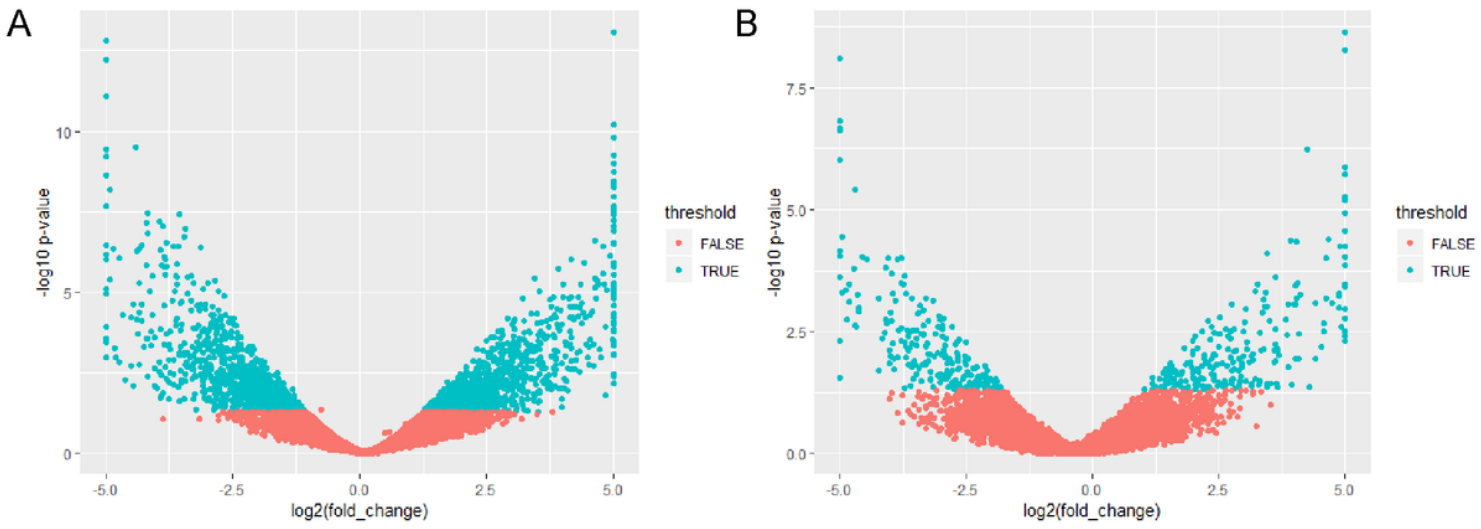

Figure 1

The volcano plot shows the overall distribution of DEmRNAs and DElncRNAs (A) DEmRNAs. (B) DElncRNAs.

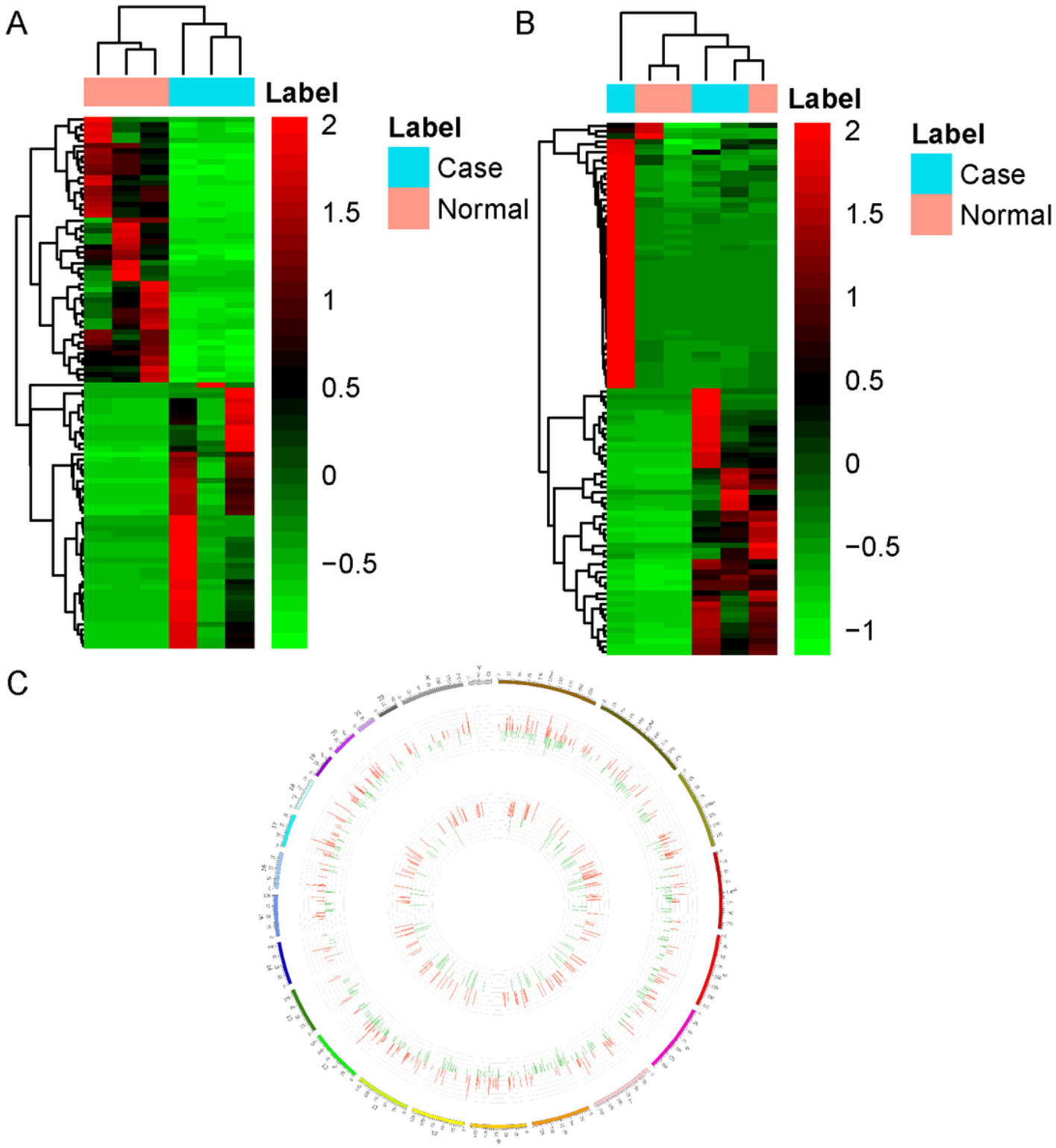

Figure 2

Heat map of the top 100 DEmRNAs and all of DElncRNAs (A) DEmRNAs. (B) DElncRNAs. Rows and columns represent DElncRNAs/DEmRNAs and tissue samples, respectively. The color scale indicates expression levels. (C) Circos plots representing the distribution of DElncRNAs and DEmRNAs on chromosomes. Red and blue colors represent up- and down-regulation, respectively.

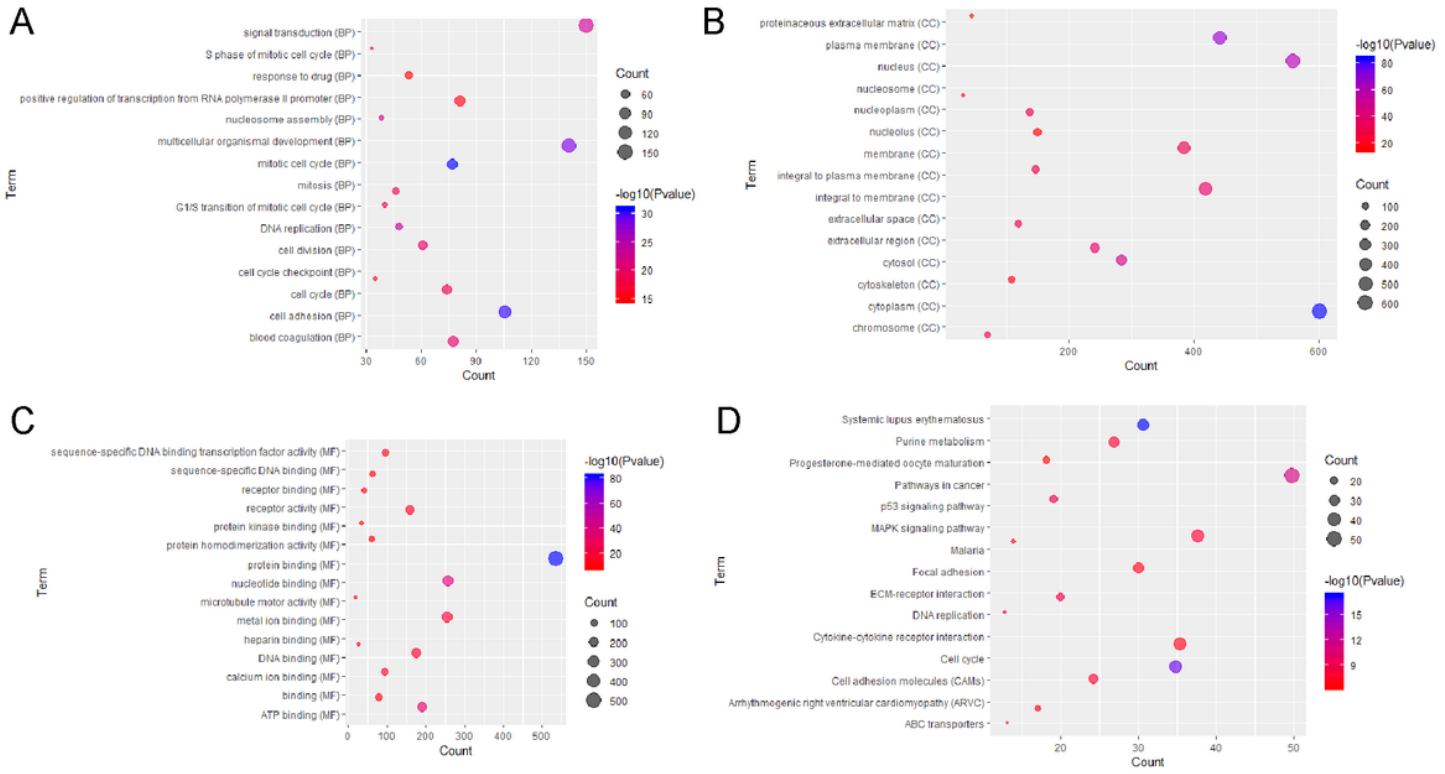

Figure 3

The top 15 significantly enriched GO terms and KEGG pathways for DEmRNAs in LUSC (A) Biological process. (B) Cellular component. (C) Molecular function. (D) KEGG pathways.

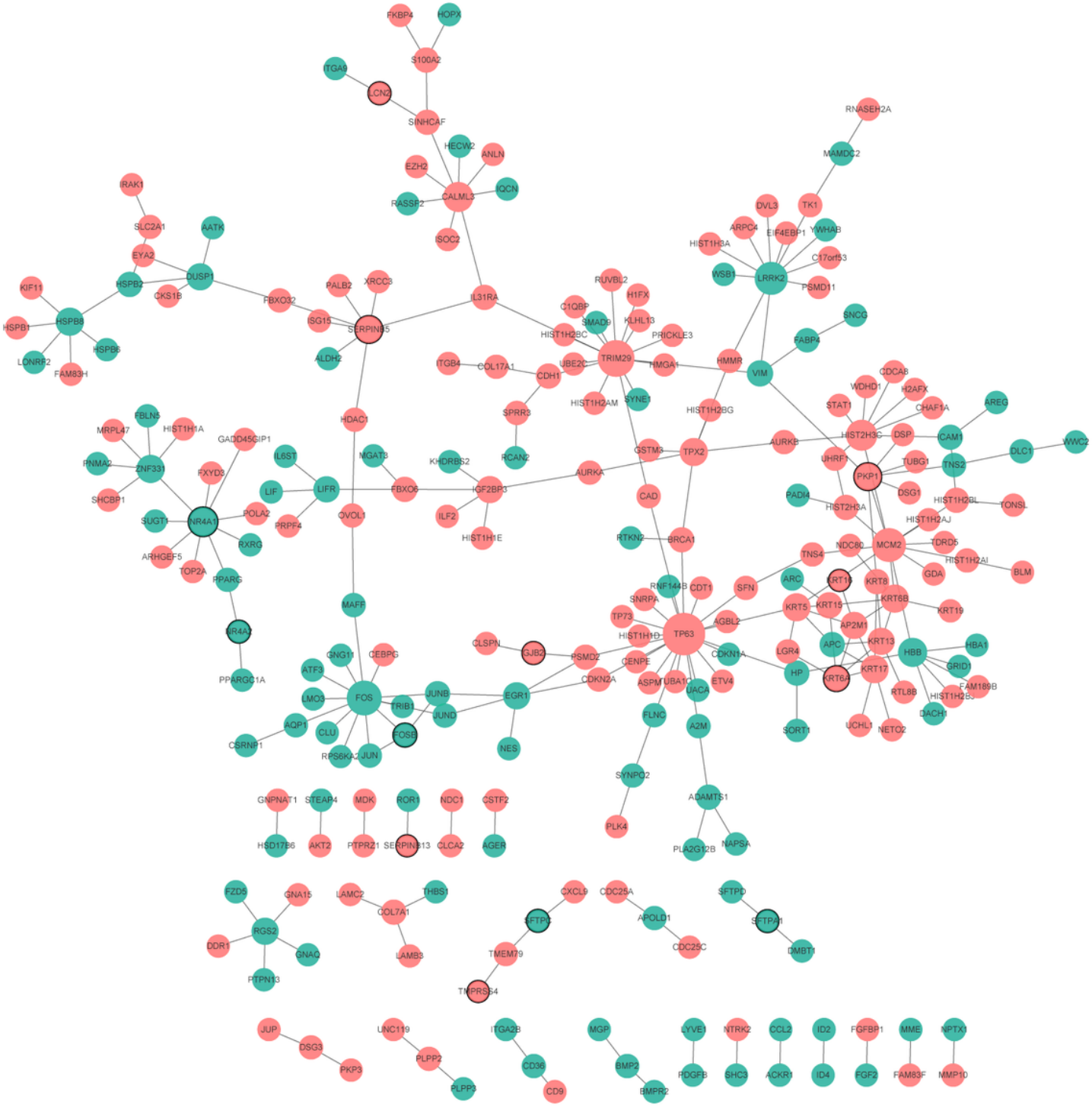

Figure 4

PPI network Ellipses are used to represent nodes, and lines are used to represent edges. Red and green represent up- and down-ward adjustments, respectively. The black border indicates the top 10 up- and down-regulated proteins. Figure 5 PPI network.

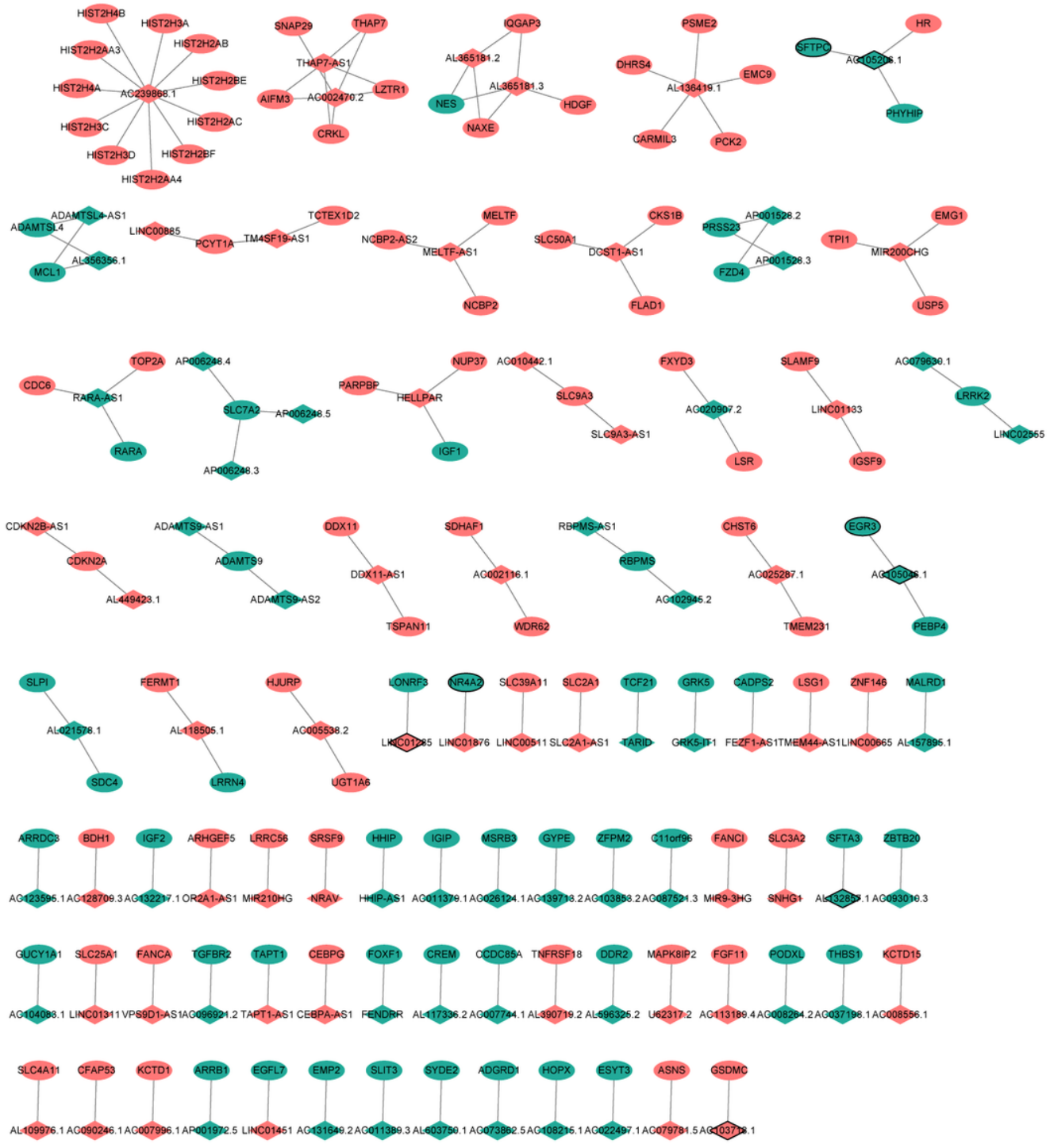

Figure 5

DElncRNA-nearby DEmRNA interaction network in LUSC Ellipses and rhombus represent DEmRNAs and DElncRNAs, respectively. Red and green colors represent up- and down-regulation, respectively. The black border indicates the top 10 up- and down-regulated DElncRNAs and DEmRNAs.

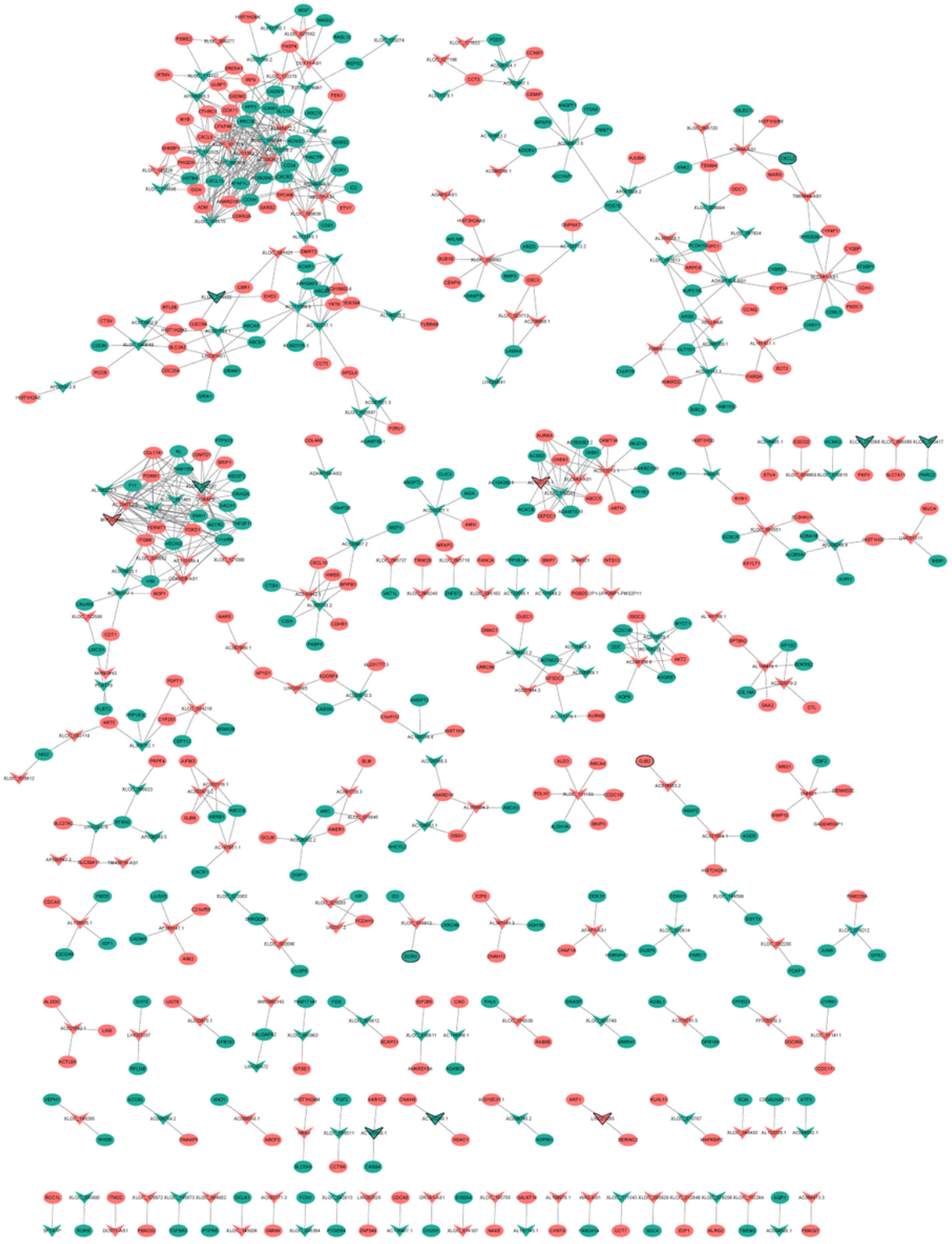

Figure 6

DElncRNA-DEmRNA co-expression in LUSC Ellipses and rhombus represent DEmRNAs and DElncRNAs, respectively. Red and green colors represent up- and down-regulation, respectively. The black border indicates the top 10 up- and down-regulated DElncRNAs and DEmRNAs.

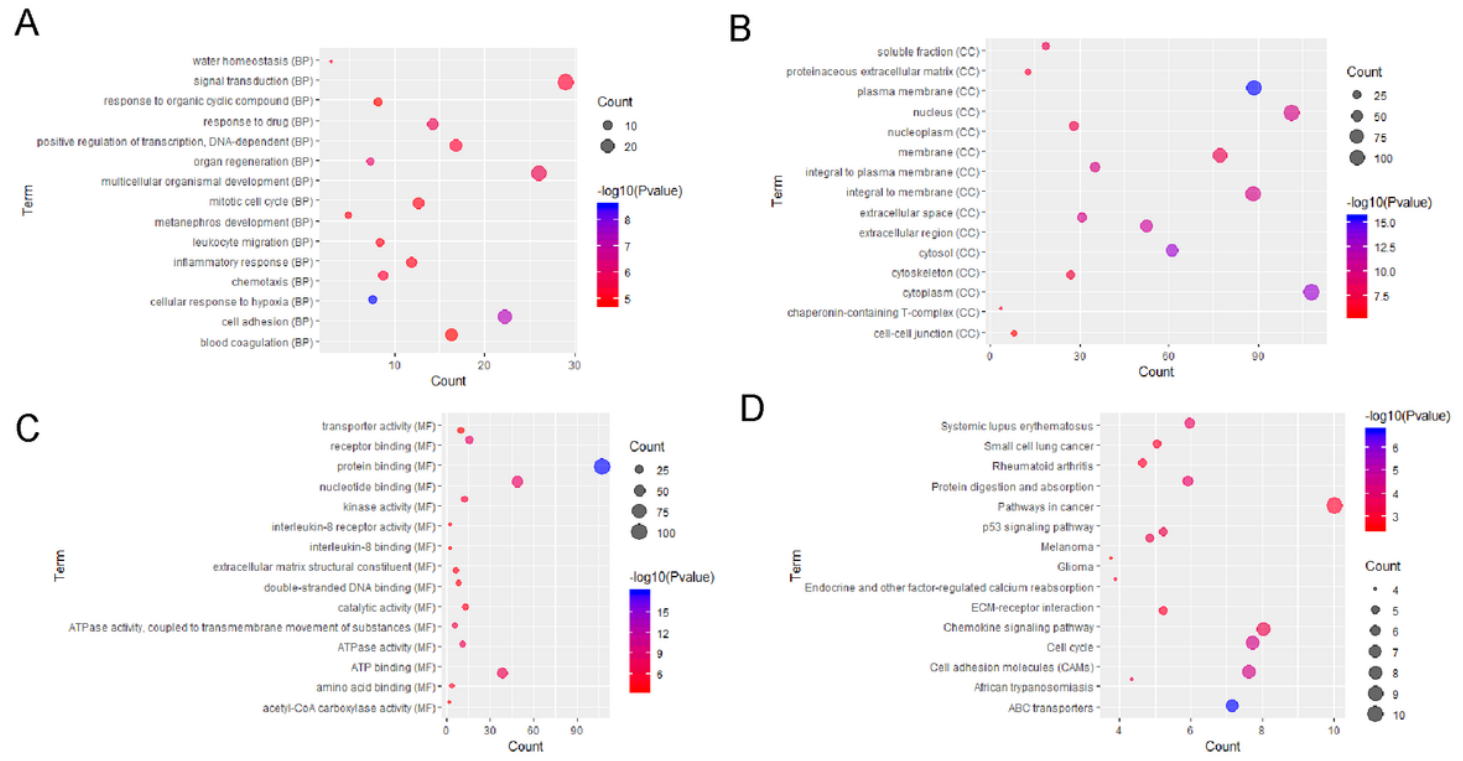

Figure 7

The top 15 significantly enriched GO terms and KEGG pathways (A) Biological process. (B) Cellular component. (C) Molecular function. (D) KEGG pathways.

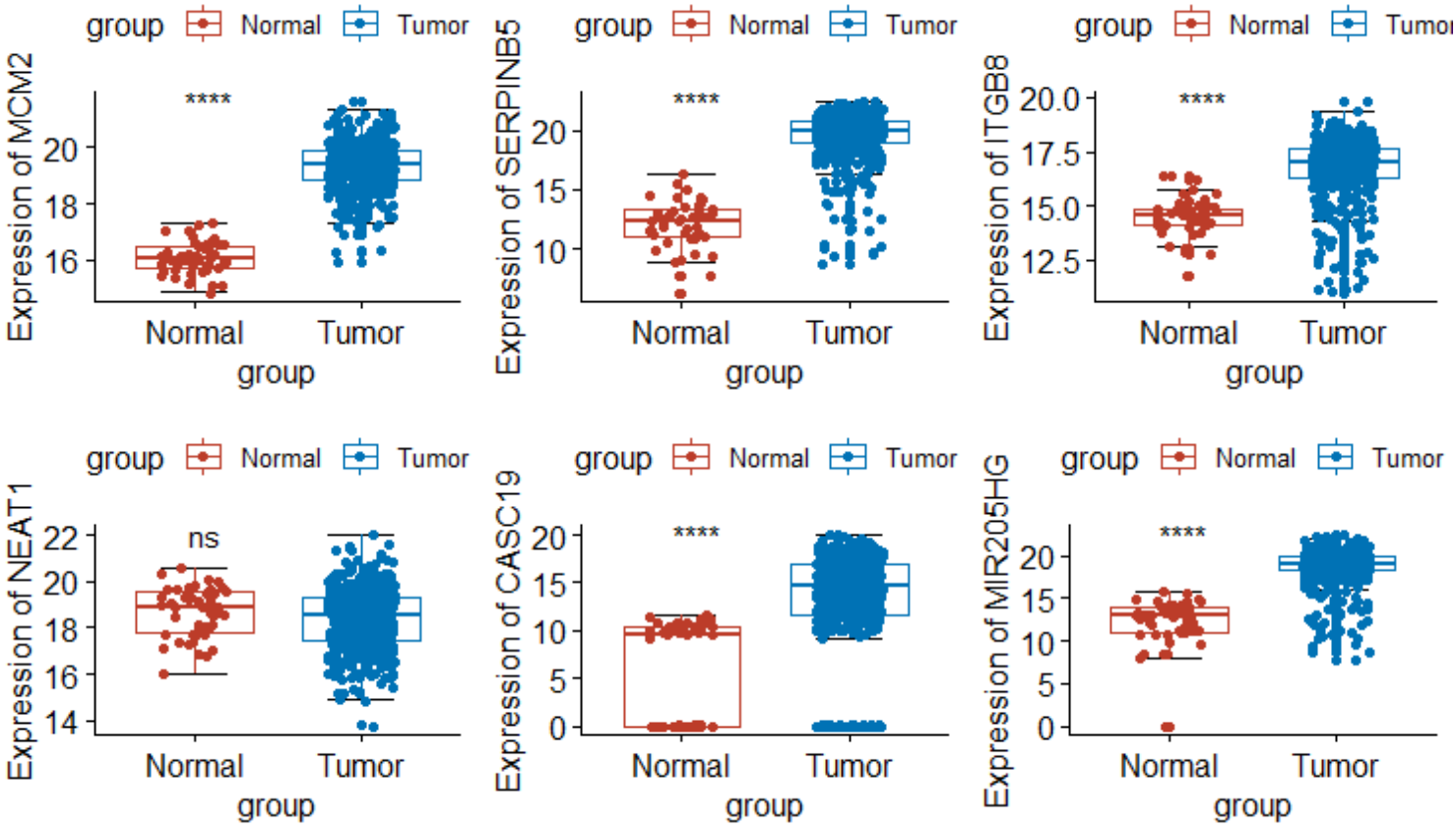

Figure 8

Validation in the TCGA dataset The x-axis shows healthy normal control (red colour) and LUSC (blue colour) groups and y-axis shows a log2 transformation to the intensities.

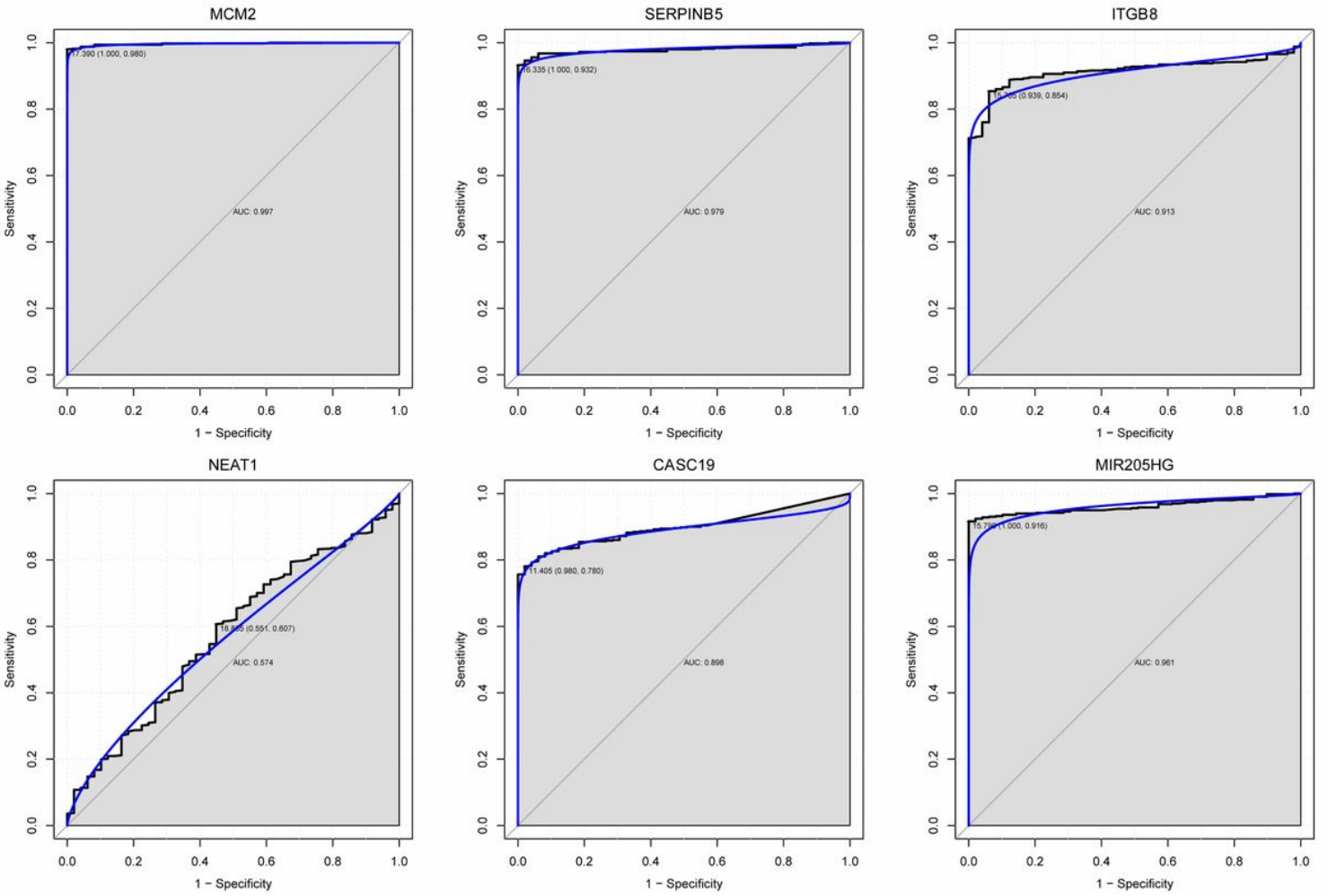

Figure 9

ROC analysis The AUC was analyzed to evaluate the performance of each DEmRNAs and DElncRNAs. The x-axis indicated 1-specificity and y-axis indicated sensitivity.

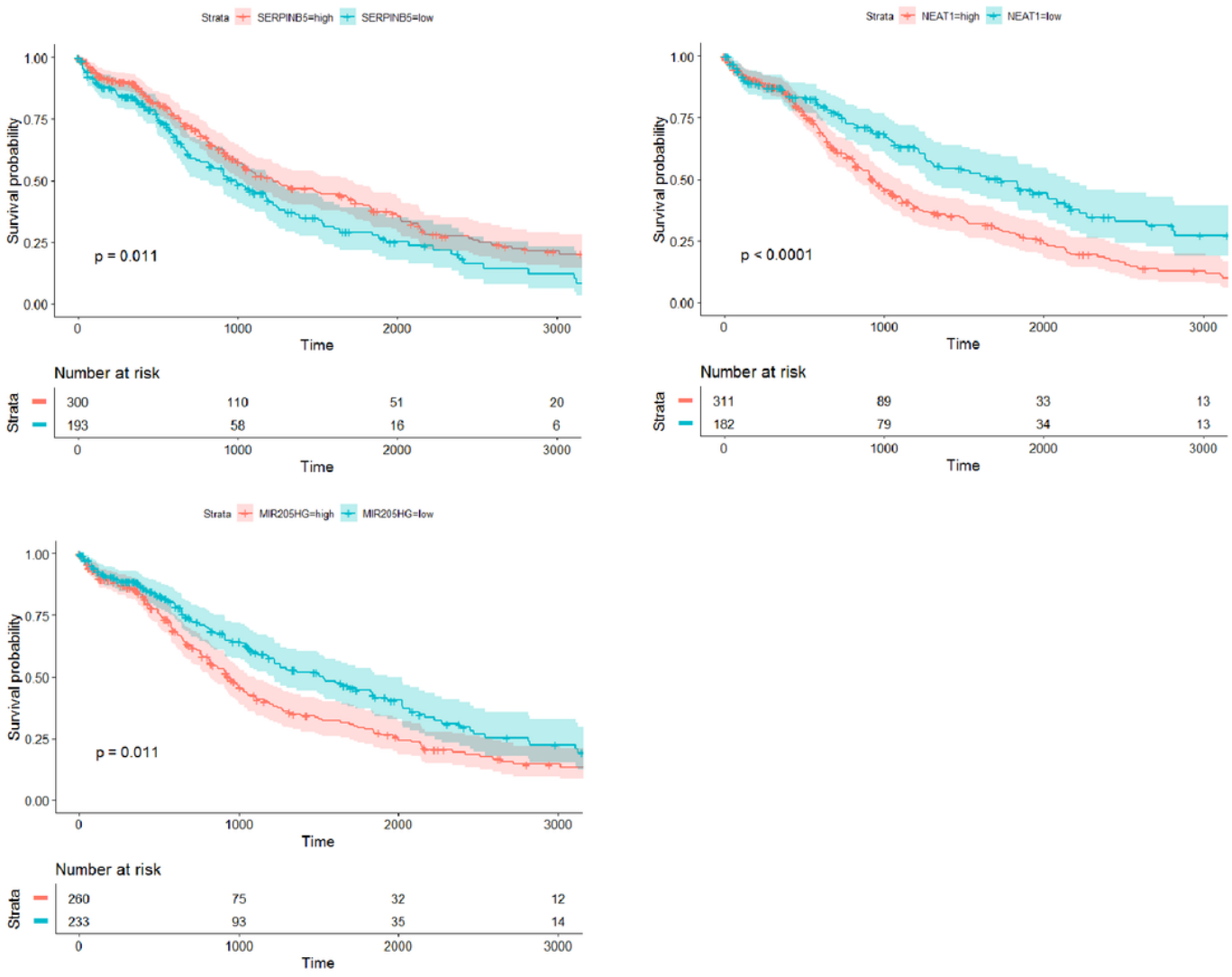

Figure 10

Survival analysis The x-axis shows times (months) and y-axis shows survival rate of patients with LUSC.

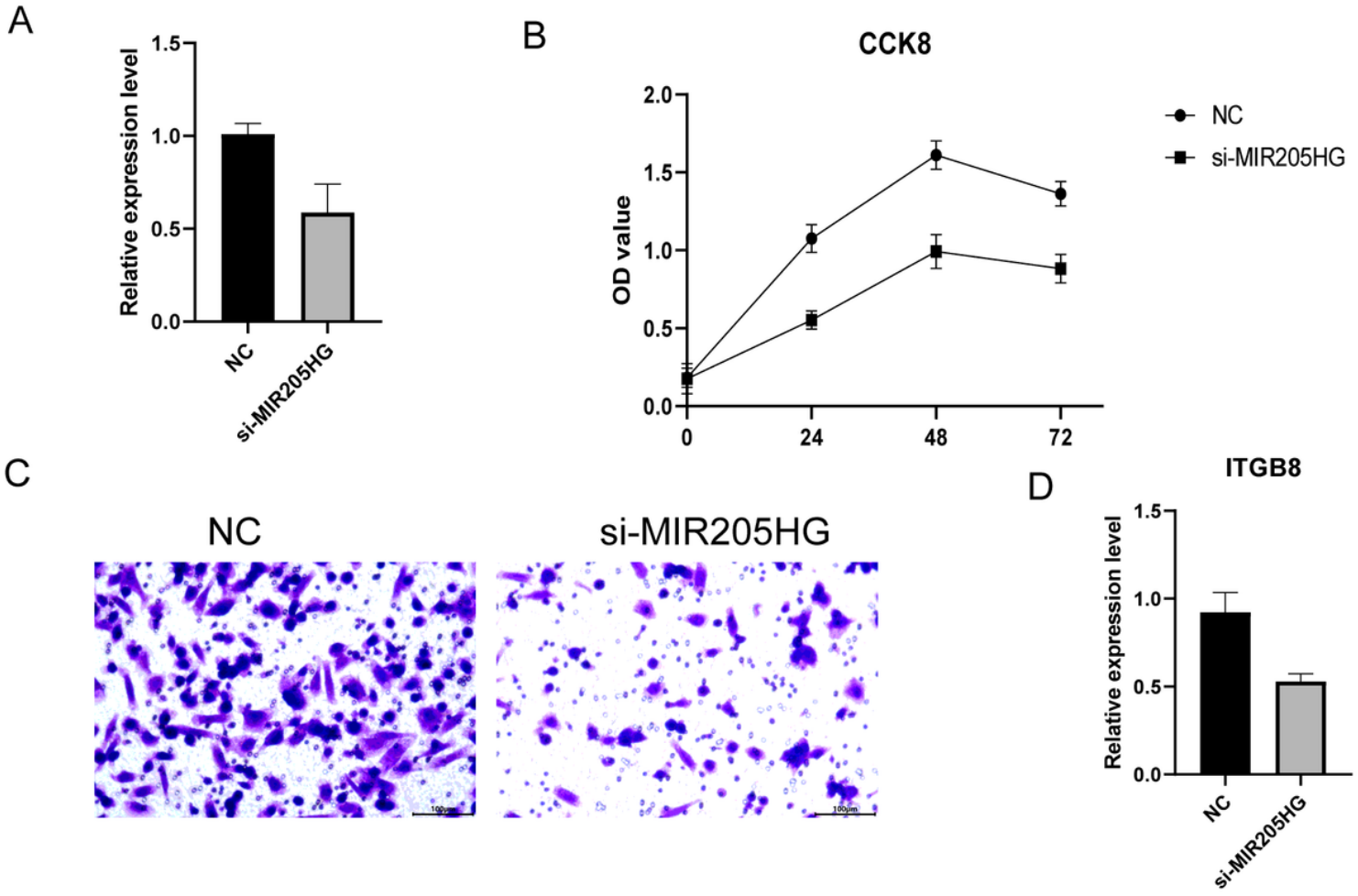

Figure 11

Knockdown of MIR205HG inhibits NCI-H520 cell proliferation and migration (A) Transfection efficacy was detected by qRT-PCR. (B) MTT assay revealed the viability of LUSC cells was suppressed by knockdown of MIR205HG. (C) Transwell assay observed the migration ability of LUSC cells was inhibited by knockdown of MIR205HG. (D) Expression of ITGB8 was detected by qRT-PCR.